JOURNAL OF CATALYSIS **165,** 80–90 (1997)
ARTICLE NO. CA971459

Intrinsic Activation Barriers as a Guide to Mechanisms of Reactions in the Gas Phase and on Solid Surfaces

Richard I. Masel[1] and Wei Ti Lee

University of Illinois, 600 S. Mathews Avenue, Urbana, Illinois 61801

Received May 14, 1996; revised August 29, 1996; accepted September 3, 1996

This paper shows that a simple heuristic, that the intrinsic barriers for C–C and C–O bond scission is 20–40 kcal/mole higher than the intrinsic barriers for C–H bond scission, provides useful insights into reactions on surfaces. Quantum mechanical calculations at various levels up to QCISD(T)/6-311G(*d*,*p*) are used to show that the gas-phase intrinsic barrier for dehydrogenation reactions of the form $\cdot H + CH_3CH_2R \rightarrow H_2 + \cdot CH_2CH_2R$ are 33 ± 2 kcal/mole less than the intrinsic barriers for hydrogenolysis reactions of the form $\cdot H + CH_3CH_2R \rightarrow CH_4 + \cdot CH_2R$ with R groups comprising a wide range of Taft parameters. We then *assume* that the difference in intrinsic barriers is the same, in the gas phase and on a surface, and use that assumption to predict mechanisms of reactions on metal surfaces. We find quite good agreement with the experiment for a wide variety of systems. In particular we explain why most hydrocarbon decomposition processes go via sequential decomposition mechanisms. We also explain why hydrogenolysis reactions have much higher activation barriers than most hydrogenation/dehydrogenation reactions on transition metal surfaces. These results imply that an examination of intrinsic barriers may provide a wide framework to characterize many types of surface reactions.

INTRODUCTION

The purpose of this paper is to suggest a simple heuristic which can be used to predict the mechanisms of reactions in the gas phase and on metal surfaces. To put this work in perspective, we as catalytic scientists all have some qualitative ideas of how reactions occur. For example, we all know that on metals hydrogenolysis reactions are more difficult than hydrogenation/dehydrogenation reactions. Reactions which break carbon–carbon, carbon–oxygen, and carbon–sulfur bonds are more difficult than reactions which break C–H bonds. Double bonds are more difficult to break than single bonds. Masel (1) has noted that one can often predict mechanisms of surface reactions, by just considering which bonds are easy or hard to break.

Yet it is also true that on some metals C–C bond scission and C–S bond scission occur readily. Consequently, even though we all know that C–C bond scission is more difficult than C–H bond scission, it is difficult to know how to apply those ideas in a quantitative way.

In this paper, we will propose some ideas that one can use to quantify the notion that some reactions are more difficult than others. We do quantum mechanical calculations to determine some of the parameters in the key equations, and use those parameters to develop heuristics which can be used to predict reaction pathways in the gas phase and on metal surfaces.

We want to say at the onset of this paper that we are not at a point where we can accurately predict mechanisms of reactions on surfaces in all cases. However, we are to the point where we can accurately predict the types of reactions which occur in many cases.

Our discussion will start with the work of Evans and Polanyi (2) almost 60 years ago. Recall that Evans and Polanyi were examining the relationship between the thermodynamics of a reaction and the activation barrier. Evans and Polanyi showed that as a reaction becomes more exothermic, its activation barrier generally decreases. Evans and Polayni also noted that in many cases E_a, the activation barrier for a given reaction is related to H_r, the heat of reaction via what is now called the Polanyi relationship

$$E_a = E_a^0 + \gamma_P \Delta H_r, \qquad [1]$$

where E_a^0 is called the intrinsic barrier to the reaction and γ_P is called the transfer coefficient. A detailed derivation of Eq. [1] is given in Masel (1). Other work has shown that γ_P is between 0.3 and 0.7 for cases of interest to catalysis (1), although γ_P can theoretically have any value. Negative values of γ_P for example arise in the so called Marcus inverted region (3).

Over the years, people have often used the Polanyi relationship to make important predictions about reactions on catalysts. Brønsted (4) used the Polanyi relationship to derive what is now called the Brønsted catalysis law. Tempkin and Pyskev (5) used the Polanyi relationship to derive the Tempkin rate equation. Balandin (6) used the Polanyi relationship to show why volcano plots arise and to derive the principle of Sabatier.

[1] To whom correspondence should be addressed.

0021-9517/97 $25.00

The interesting thing though is that very little work has been done to understand how variations in the intrinsic barriers to reaction affect the activation barriers to surface reactions. Masel (1) noted that the intrinsic barriers may be a way to quantify the idea that some elementary reactions are more difficult than others. Note that according to Eq. [1] the activation barrier for a given elementary surface reaction is given by the intrinsic barrier to reaction plus a correction due to the thermodynamic driving force for the reaction. If everything else is equal, an elementary reaction with a low intrinsic barrier will be less difficult than an elementary reaction with a high intrinsic barrier. Therefore, the intrinsic barriers to reaction are a quantitative measure of whether some reactions are more difficult than others. Later in this paper we will also show that an examination of the intrinsic barriers to reaction also allow one to predict whether one reaction pathway is favored over another reaction pathway. Therefore the intrinsic barrier can be thought of as a way to quantify the idea that some reactions are more difficult than others.

There is a twofold advantage to using the intrinsic barrier to quantify how difficult reactions are: (1) one can calculate the intrinsic barriers exactly in the gas phase using quantum mechanical calculations, and (2) one can use the results of the calculations to make useful predictions. In particular, if one knows the intrinsic barrier, and uses a correlation for the heat of reaction one can predict reaction mechanisms. Therefore, a knowledge of intrinsic barriers is quite useful.

In this paper we will use *ab initio* calculations to evaluate the intrinsic barriers for a number of dehydrogenation and hydrogenolysis reactions. We will then use that information to attempt to predict mechanisms of reactions in the gas phase and on metal surfaces.

THE ORIGIN OF THE INTRINSIC BARRIERS TO REACTION

Intrinsic barriers have been extensively discussed in the theoretical organic chemistry literature, but many of the ideas have not been extensively discussed in the catalytic literature. Therefore, it is useful to start the discussion by considering why there is an intrinsic barrier to a reaction. Let us consider a simple reaction

$$AB + C \rightarrow A + BC \qquad [2]$$

When reaction 2 occurs A–B bond stretches and breaks. Simultaneously the B–C bond forms. It costs energy to stretch the A–B bond. However, the system gains energy as the B–C bond forms. If, at every point during the reaction, the energy gain due to B–C bond formation exceeds the energy loss due to A–B bond destruction, and there are no extra repulsions, the reaction will not be activated. Thus, one needs to do some analysis before one can say whether a given reaction will have a significant activation barrier.

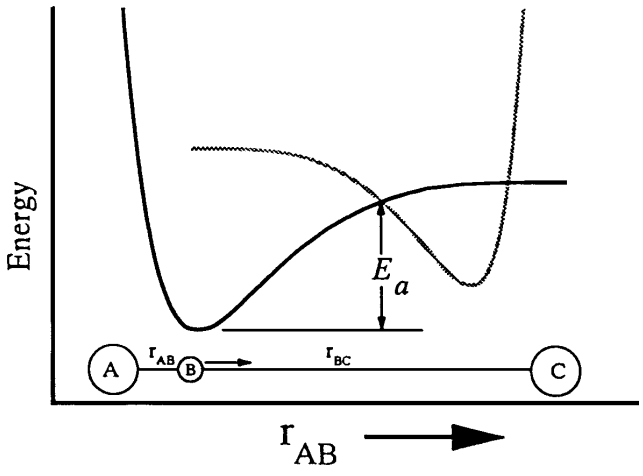

FIG. 1. A schematic of a 1-D potential energy curve for the reaction $AB + C \rightarrow A + BC$, using Morse potentials.

Evans and Polanyi (2) and Marcus (7) proposed that one can estimate the activation barrier for a reaction in the form in [2] by considering the formation of the A–B bond and the destruction of the B–C bond separately. Following Evans and Polanyi, we will assume that during the reaction atom B is transferred from atom A to atom C. We will write the total energy of the system as the sum of two energies: the energy of the A–B bond and the energy of the B–C bond. Further, we will assume that the energy of the A–B and B–C bonds is given by Morse potentials as shown in Fig. 1. Now, for the purposes of discussion assume that we are transferring atom B from A to C in the linear geometry shown on the bottom of Fig. 1. During the reaction, the A–B bond stretches, while the B–C bond forms. The energy of the A–B bond moves up the Morse potential on the left side of Fig. 1, while the energy of the B–C bond moves down the Morse potential on the right side of Fig. 1. Notice that in the initial part of the reaction, the energy of the A–B bond goes up more than the energy of the B–C bond goes down. The net effect is that the energy of the system goes up. However, later in the reaction the B–C bond starts to form so the energy of the system goes down again. As a result, the reaction is activated.

This example suggests that activation barriers to reaction arise because bonds in the reactants need to stretch or be distorted before new bonds can form. One can show that the intrinsic barrier to reaction is equal to the energy it takes to stretch or distort the orbitals in the reactants so that new bonds can form. Consequently, the intrinsic barrier is a critical factor in determining the activation barriers for a reaction. Physically, as the orbital distortion increases, the activation barriers to reaction increase. That makes it harder for a reaction to occur.

When one actually does quantum mechanical calculations, one finds that idealized curves in Fig. 1 are not quite correct. Instead, the potential contour follows the upper

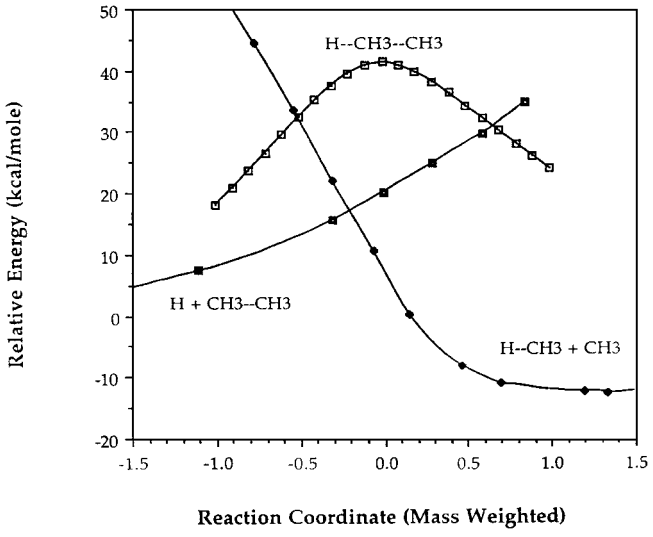

FIG. 2. An actual potential energy curve for the methyl transfer reaction, determined from IRC calculations. The C–H and C–C potentials are also included such that the C–H and C–C bond lengths match those on the actual potential energy curve.

curve in Fig. 2. There are electron–electron repulsions when the reactants first come together. The electron–electron repulsions raise the intrinsic barriers to reactions. There is state mixing at the curve crossing in Fig. 1. State mixing lowers the intrinsic barriers. Thus Fig. 1 is not quite correct. Nevertheless, one can still view the intrinsic barrier as a measure of the bond distortions that happen when reaction occurs. It is just that some of the bond distortions occur because of long-range electron–electron repulsions, state mixing, and other quantum effects.

QUANTUM MECHANICAL CALCULATIONS OF THE INTRINSIC BARRIERS TO REACTION IN THE GAS PHASE

One of the advantages of thinking about intrinsic barriers is that one can use quantum mechanical calculations to evaluate the intrinsic barriers for many reactions. In this paper we report results of quantum mechanical calculations of the intrinsic barriers for a number *gas phase* dehydrogenation reactions of the form

$$H\cdot + CH_3CH_2R \rightarrow HH + \cdot CH_2CH_2R \qquad [3]$$

and a number of *gas phase* hydrogenolysis reactions of the form

$$H\cdot + CH_3CH_2R \rightarrow CH_4 + \cdot CH_2R \qquad [4]$$

with R = H, CH_3, NH_2, CF_3, CN, and C_6H_5.

CALCULATIONAL METHODS

The calculations reported here were all done with the GAUSSIAN suite of programs. Geometries of equilibrium structures were fully optimized at the second-order Moller–Plesset perturbation theory (MP2) using a double valence basis set with *d*-polarization function added to the heavy atoms (6-31G(*d*)). A polarization function (*p*-type) was also added to hydrogen atoms when optimizing the structures of transition states because long C–H and H–H bonds were involved.

Single point calculations at fourth-order Moller–Plesset perturbation theory (UMP4) and quadratic configuration interaction (QCISD(T)) were carried out to accurately account for the correlation energies. These high-level calculations were done using a triple valence basis sets supplemented with polarization functions to all atoms (6-311G(*d*,*p*)). We have also done calculations using the G-2 theory (8) which has been shown to have accuracy within 1–2 kcal/mole of experimental values. G-2 calculations is a theory based on PMP4/6-311 G(*d*,*p*) energies with a number of corrections including diffuse functions, higher polarization functions and zero point energies.

Calculations were also performed with various basis sets ranging from STO-3G to 6-311++G(*d*,*p*) at the PMP2 level to study the effects of basis sets on the optimized transition geometries, heats of reactions, and activation energies. Since we are dealing with transition states that have large bond distances and open shell structures, spin projection (9) was used in the calculations to correct for spin contamination. Frequency calculations were also done to make sure that the transition states found were actually first-order saddle points with one imaginary frequency. We did not make any corrections for the basis-set superposition errors. Such corrections would be in the order of 1–2 kcal/mole for all of the examples here. All the calculations were performed using the GAUSSIAN92 (10) and GAUSSIAN94 (11) programs.

The values of transfer coefficient in the Polanyi relationship were determined from the slopes of the reaction pathway based on Bockris' method (12). Intrinsic reaction coordinate (IRC) calculations (13) were carried out to trace the reaction path leading down from the transition state toward the reactants and products. The slopes at the inflection points of the energy vs. reaction coordinate plot were then used to determine the transfer coefficients as described previously (14).

CALCULATIONAL RESULTS

Figure 3 shows the transition state geometries considered in this paper. For the dehydrogenation reaction, reaction 3, it was assumed that the hydrogen atom attacks the alphatrans hydrogen of the CH_3CH_2R molecule along the C–H axis, as depicted in Fig. 3(b). C_s symmetry was used in most of the calculation. However, we have done calculations without the symmetry, and found no change in the structures and energies of the transition states. For

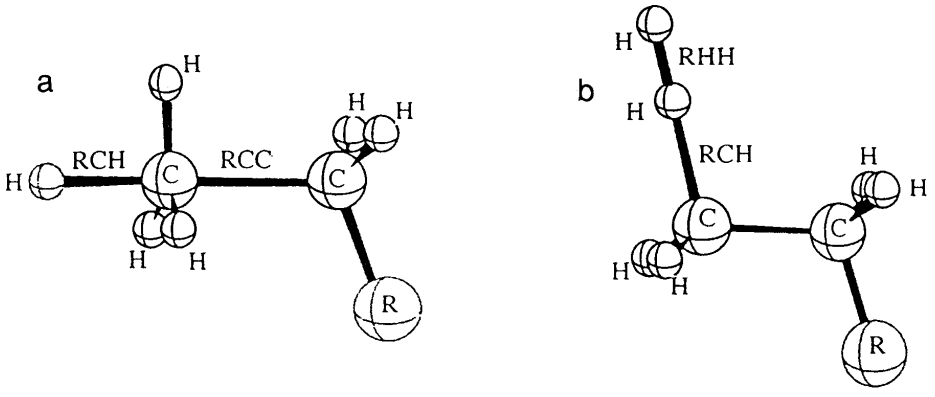

FIG. 3. The transition state structures considered in this paper, (a) the methyl transfer reactions, (b) the hydrogen transfer reactions.

the dehydrogenolysis reaction, reaction 4, the hydrogen atom was assumed to approach the CH_3CH_2R molecule along the C–C axis. C_s symmetry was also used in this reaction. Again, no change in the structures and energies was found when the symmetry was relaxed. We have also looked at the case when the hydrogen atom attacks perpendicular to the C–C bond. However, we found that the activation barriers were larger in this geometry. Table 1 provides the optimized bond lengths of the forming and breaking bonds of the transition states. Generally, the larger the basis set, the bond lengths are shorter. It was also found that the polarization function added to the hydrogen is essential when doing geometry optimization of the transition states.

Tables 2 and 3 list the energies calculated at the PMP4, QCISD(T) and G-2 level. The inclusion of more electron correlation tends to lower the activation energies, and moves the heats of reaction to be more exothermic. However, due to the cancellation of errors, the calculated intrinsic activation energies are relatively constant over the different levels of calculations. It is also interesting to find that the intrinsic activation energies stay rather constant over the different R groups of each reaction. The intrinsic activation energies are around 46 kcal/mole and 13 kcal/mole for the hydrogenolysis and dehydrogenation reactions, respectively.

We have also investigated the effects of different basis sets on the values of intrinsic activation energies for the case when the R group is H. The results are summarized in Tables 4 and 5. Similar to the inclusion of electron correlation, we found that larger basis sets tend to lower the activation energies which make the heats of reaction more

TABLE 1

Selected Transition State Bond Lengths for the Hydrogen Transfer and Methyl Transfer Reactions Optimized at Various Basis Sets at PMP2 Level

		Hydrogen transfer reaction		Methyl transfer reaction	
R Group	Method/Basis	RHH	RCH	RCH	RCC
H	PMP2/6-31G(*d*)	0.892	1.405	1.383	1.875
	PMP2/6-31G(*d*,*p*)	0.890	1.378	1.369	1.853
	PMP2=(FULL)/6-31G(*d*,*p*)	0.889	1.379	1.368	1.852
	PMP2/6-31+G(*d*,*p*)	0.889	1.378	1.367	1.851
	PMP2/6-311G(*d*,*p*)	0.888	1.386	1.364	1.855
CH_3	PMP2=(FULL)/6-31G(*d*,*p*)	0.886	1.383	1.372	1.846
	PMP2/6-31+G(*d*,*p*)	0.886	1.383	1.371	1.845
	PMP2/6-311G(*d*,*p*)	0.885	1.392	1.367	1.848
NH_2	PMP2=(FULL)/6-31G(*d*,*p*)	0.887	1.384	1.402	1.849
	PMP2/6-31+G(*d*,*p*)	0.887	1.385	1.400	1.844
CF_3	PMP2=(FULL)/6-31G(*d*,*p*)	0.880	1.389	1.364	1.845
	PMP2/6-31+G(*d*,*p*)	0.881	1.387	1.365	1.851
CN	PMP2=(FULL)/6-31G(*d*,*p*)	0.879	1.391	1.349	1.838
	PMP2/6-31+G(*d*,*p*)	0.878	1.392	1.348	1.837
C_6H_5	PMP2/6-31+G(*d*,*p*)	0.884	1.388	1.368	1.832

TABLE 2

The Activation Energies, Heats of Reactions, Transfer Coefficients, and Intrinsic Barriers for the Methyl Transfer Reaction Calculated at the PMP2, PMP4 (SDTQ), and QCISD(T) Levels

R Group	Level of calculation	Energies (Hartrees) H	Energies (Hartrees) CH_3CH_2R	T.S.	CH_4	CH_2R	E_a (kcal/mol)	ΔH_r (kcal/mol)	γ_P	E_a^0
H	PMP2	−0.49981	−79.57089	−80.00725	−40.37923	−39.70917	39.81	−11.11	0.59	46.37
	UMP4(SDTQ)	−0.49981	−79.61452	−80.04794	−40.40503	−39.73077	41.66	−13.47	0.59	49.61
	QCISD(T)	−0.49981	−79.61579	−80.05258	−40.40589	−39.73224	39.55	−14.14	0.59	47.89
CH_3	PMP2	−0.49981	−118.76605	−119.20440	−40.37923	−78.90507	38.56	−11.57	0.58	45.28
	UMP4(SDTQ)	−0.49981	−118.82727	−119.26263	−40.40503	−78.94459	40.44	−14.14	0.58	48.64
	QCISD(T)	−0.49981	−118.82879	−119.26743	−40.40589	−78.94663	38.39	−15.01	0.58	47.10
NH_2	PMP2	−0.49981	−134.78617	−135.22848	−40.37923	−94.93576	36.08	−18.20	0.55	46.10
	UMP4(SDTQ)	−0.49981	−134.84186	−135.28120	−40.40503	−94.96935	37.95	−20.52	0.55	49.24
	QCISD(T)	−0.49981	−134.84289	−135.28576	−40.40589	−94.97126	35.73	−21.62	0.55	47.62
CN	PMP2	−0.49981	−171.60175	−172.04305	−40.37923	−131.74610	36.71	−14.92	0.61	45.82
	UMP4(SDTQ)	−0.49981	−171.66086	−172.09737	−40.40503	−131.77787	39.72	−13.95	0.61	48.23
	QCISD(T)	−0.49981	−171.65759	−172.09987	−40.40589	−131.78318	36.10	−19.88	0.61	48.23
CF_3	PMP2	−0.49981	−416.01715	−416.45479	−40.37923	−376.14852	39.01	−6.77	0.59	43.00
	UMP4(SDTQ)	−0.49981	−416.08450	−416.51933	−40.40503	−376.19390	40.78	−9.18	0.59	46.19
	QCISD(T)	−0.49981	−416.08122	−416.51916	−40.40589	−376.19129	38.83	−10.14	0.59	44.81

Note. 6-311G(*d*,*p*) basic set was used.

exothermic.This is probably due to the fact that electron correlation and larger basis functions lower the energy of the transition states more than that of the reactants and products. Polarization functions are found to be important in getting reliable values for both the activation energies and heats of reactions. Diffuse functions do not appear to affect the energies significantly. It is also found that the transfer coefficient does not depend on the types of basis function used in the IRC calculations.

DISCUSSION

Looking back to the results in Tables 2 and 3 allows one to draw some interesting conclusions about the relative

TABLE 3

The Activation Energies, Heats of Reactions, Transfer Coefficients, and Intrinsic Barriers for the Hydrogen Transfer Reaction Calculated at PMP2, PMP4(SDTQ), and QCISD(T) Levels

R Group	Level of calculation	Energies (Hartrees) H	Energies (Hartrees) CH_3CH_2R	T.S.	H_2	CH_2R	E_a (kcal/mol)	ΔH_r (kcal/mol)	γ_P	E_a^0
H	PMP2	−0.49981	−79.57089	−80.04707	−1.16027	−78.90507	14.83	3.36	0.70	12.48
	UMP4(SDTQ)	−0.49981	−79.61452	−80.09082	−1.16772	−78.94459	14.76	1.27	0.70	13.87
	QCISD(T)	−0.49981	−79.61579	−80.09399	−1.16832	−78.94663	13.56	0.41	0.70	13.27
CH_3	PMP2	−0.49981	−118.76605	−119.24177	−1.16027	−118.09931	15.11	39.4	0.71	12.32
	UMP4(SDTQ)	−0.49981	−118.82727	−119.30310	−1.16772	−118.15657	15.05	1.75	0.71	13.81
	QCISD(T)	−0.49981	−118.82879	−119.30655	−1.16832	−118.15895	13.83	0.83	0.71	13.24
NH_2	PMP2	−0.49981	−134.78617	−135.26180	−1.16027	−134.11939	15.18	3.97	0.71	12.36
	UMP4(SDTQ)	−0.49981	−134.84186	−135.31785	−1.16772	−134.17124	14.95	1.70	0.71	13.74
	QCISD(T)	−0.49981	−134.84289	−135.32096	−1.16832	−134.17338	13.64	0.63	0.71	13.19
	G2 procedures	−0.50000	−134.89457	−135.37672	−1.16637	−134.23304			0.71	13.36
CN	PMP2	−0.49981	−171.60175	−172.07526	−1.16027	−170.93262	16.50	5.44	0.72	12.58
	UMP4(SDTQ)	−0.49981	−171.66086	−172.13468	−1.16722	−170.98785	16.31	3.19	0.72	14.01
	QCISD(T)	−0.49981	−171.65759	−172.13346	−1.16832	−170.98549	15.03	2.26	0.72	13.40
CF_3	PMP2	−0.49981	−416.01715	−416.49055	−1.16027	−415.34879	16.32	4.95	0.73	12.70
	UMP4(SDTQ)	−0.49981	−416.08450	−416.55862	−1.16722	−415.41217	16.12	2.77	0.73	14.10
	QCISD(T)	−0.49981	−416.08122	−416.55730	−1.16637	−415.40979	14.89	3.06	0.73	12.66

Note. 6-311G(*d*,*p*) basic set was used.

TABLE 4

The Energetics for the Methyl Transfer Reaction When the R Group is H, Calculated at Various Basis Sets at the PMP2 Level

Method/Basis set	PMP2 Energies (Hartrees) H	PMP2 Energies (Hartrees) CH_3CH_2	T.S.	HCH_3	CH_3	E_a (kcal/mol)	ΔH_r (kcal/mol)	γ_P	E_a^0
PMP2/STO-3G	−0.46658	−78.41333	−78.79314	−39.78307	−39.11759	54.45	−13.02	(0.59)	62.13
PMP2/6-31G	−0.49823	−79.38560	−79.81426	−40.27913	−39.62385	43.66	−12.01	0.54	50.15
PMP2/6-31G(*d*)	−0.49823	−79.49474	−79.91905	−40.32255	−39.67075	46.39	−0.20	0.60	46.51
PMP2/6-31G(*d*,*p*)	−0.49823	−79.54340	−79.97349	−40.36463	−39.69462	42.76	−11.05	0.59	49.28
PMP2/6-31+g(*d*,*p*)	−0.49823	−79.54579	−79.97825	−40.36595	−39.69813	41.28	−12.59	0.59	48.70
PMP2/6-31++G(*d*,*p*)	−0.49880	−79.54617	−79.97906	−40.36611	−39.69833	41.36	−12.21	0.59	48.57
PMP2/6-311G(*d*)	−0.49981	−79.52592	−79.95476	−40.34934	−39.68679	44.53	−6.53	0.60	48.45
PMP2/6-311G(*d*,*p*)	−0.49981	−79.57089	−80.00725	−40.37923	−39.70917	39.81	−11.11	0.58	46.26
PMP2/6-311+G(*d*,*p*)	−0.49981	−79.57148	−80.00845	−40.37953	−39.71041	39.43	−11.70	(0.59)	46.33
PMP2/6-31++G(*d*,*p*)	−0.49982	−79.57167	−80.00885	−40.37964	−39.71054	39.31	−11.73	(0.59)	46.23
PMP2/D95(*d*)	−0.49764	−79.49797	−79.92428	−40.33441	−39.67495	44.76	−8.63	(0.59)	49.85
PMP2/D95(*d*,*p*)	−0.49764	−79.54877	−79.98061	−40.36768	−39.69983	41.29	−13.24	(0.59)	49.10
PMP2/D95+(*d*,*p*)	−0.49764	−79.55228	−79.98654	−40.36937	−39.70136	39.77	−13.06	(0.59)	47.47
PMP2/D95++(*d*,*p*)	−0.49922	−79.55335	−79.98781	−40.36972	−39.70166	40.64	−11.81	(0.59)	47.60

barriers of dehydrogenation and hydrogenolysis reactions. Notice that at the QCISD(T) level of the calculation (the most accurate) the intrinsic barriers to all of the dehydrogenation reactions examined here are in the order of 13 kcal/mole while the intrinsic barriers to all of the hydrogenolysis reactions considered here are on the order of 45 kcal/mole. Therefore, it seems that in the gas phase, the intrinsic barrier to C−H bond scission is much lower than the intrinsic barrier to C−C bond scission.

It is easy to understand why the intrinsic barriers to C−H bond scission are so much lower than the intrinsic barriers to C−C bond scission. Consider the dehydrogenation and hydrogenolysis of ethane. Figure 4 shows the how the geometry of ethane changes during the hydrogen transfer reaction. Our calculations show that the lowest barrier for hydrogen transfer occurs when the incoming hydrogen approaches the ethane along the C−H bond. The C−H bond extends, and a new H−H bond forms in qualitative agreement with the results in Fig. 1.

In contrast, Fig. 5 shows the best geometry for the hydrogenolysis of ethane. During the reaction the hydrogen approaches the C−H group along the C−C bond axis. The

TABLE 5

The Energetics for the Hydrogen Transfer Reaction When the R Group is H, Calculated at Various Basis Sets at the PMP2 Level

Method/Basis set	PMP2 Energies (Hartrees) H	PMP2 Energies (Hartrees) CH_3CH_3	T.S.	H_2	CH_2CH_3	E_a (kcal/mol)	ΔH_r (kcal/mol)	γ_P	E_a^0
PMP2/STO-3G	−0.46658	−78.41333	−78.85270	−1.13014	−77.75417	17.08	−2.76	(0.70)	19.01
PMP2/6-31G	−0.49823	−79.38560	−79.85526	−1.14414	−78.73476	17.93	−3.10	0.69	15.80
PMP2/6-31G(*d*)	−0.49823	−79.49474	−79.96111	−1.14414	−78.83772	20.00	6.98	(0.70)	15.11
PMP2/6-31G(*d*,*p*)	−0.49823	−79.54340	−80.01553	−1.15766	−78.87794	16.38	3.79	0.70	13.73
PMP2/6-31+g(*d*,*p*)	−0.49823	−79.54579	−80.01837	−1.15766	−78.88231	16.10	2.54	0.69	14.34
PMP2/6-31++G(*d*,*p*)	−0.49880	−79.54617	−80.01990	−1.15777	−78.88277	15.73	2.78	(0.70)	13.78
PMP2/6-311G(*d*)	−0.49981	−79.52592	−79.99401	−1.14588	−78.86795	19.90	7.46	(0.70)	14.68
PMP2/6-311G(*d*,*p*)	−0.49981	−79.57089	−80.04707	−1.16027	−78.90507	14.83	3.36	0.70	12.48
PMP2/6-311+G(*d*,*p*)	−0.49981	−79.57148	−80.04787	−1.16027	−78.90666	14.70	2.74	(0.70)	12.78
PMP2/6-311++G(*d*,*p*)	−0.49982	−79.57167	−80.04832	−1.16030	−78.90688	14.54	2.70	(0.70)	12.65
PMP2/D95(*d*)	−0.49764	−79.49797	−79.96359	−1.14391	−78.84254	20.09	5.75	(0.70)	16.06
PMP2/D95(*d*,*p*)	−0.49764	−79.54877	−80.02086	−1.15873	−78.88475	16.03	1.84	(0.70)	14.74
PMP2/D95+(*d*,*p*)	−0.49764	−79.55228	−80.02595	−1.15873	−78.88822	15.04	1.86	(0.70)	13.73
PMP2/D95++(*d*,*p*)	−0.49922	−79.55335	−80.02789	−1.15873	−78.88909	15.49	2.98	(0.70)	13.40

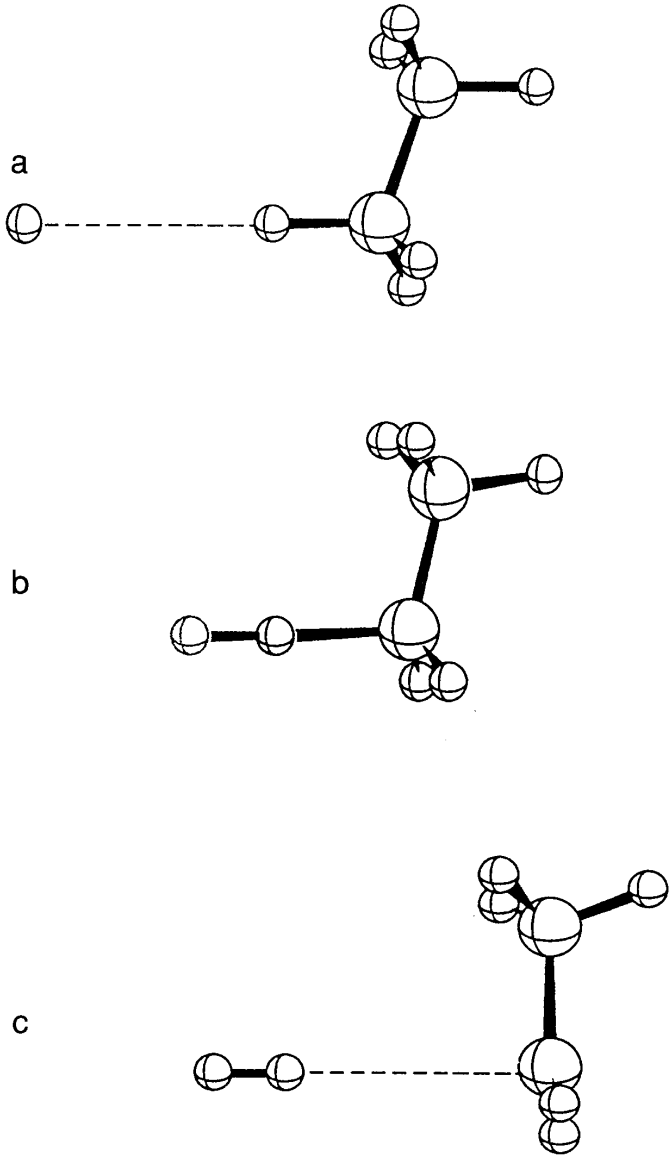

FIG. 4. The progress of the hydrogen transfer reaction, $H + C_2H_6 \rightarrow HH + C_2H_5$.

C–C bond breaks, and a new C–H bond forms. Simultaneously, the umbrella of the other three hydrogens on the CH_3 inverts into the final geometry. It costs energy to flip the CH_3 group. There also are strong Pauli repulsions between the incoming hydrogen and the hydrogens on the methyl group. Consequently, the intrinsic activation barrier for C–C bond scission is considerably higher than the intrinsic barrier to C–H bond scission.

We have also considered the possibility of a hydrogenolysis reaction occurring where a hydrogen atom approaches perpendicularly to the ethane as shown in Fig. 6. One can imagine a transition state for the reaction like that in Fig. 6b, where the C–C bonds are breaking and the C–H bonds are forming. In fact, however, the bonding in Fig. 6b is quantum mechanically forbidden (one is putting three electrons into a single molecular orbital). One would have to break bonds before new bonds can form. Therefore, the intrinsic barriers to this reaction would be expected to be high. Our quantum mechanical calculations indicate that the intrinsic barrier to reaction at the geometry in Fig. 6 is almost 68 kcal/mole, i.e., 22 kcal/mole higher than the reaction in Fig. 5.

The results in this paper also show that the intrinsic barrier only changes moderately as one changes the R group. Figure 7 shows a plot of the intrinsic barriers for C–H and C–C bond scission as a function of the Taft parameter for the R-group. Notice that the intrinsic barriers are essentially constant over a wide range of Taft parameters. Therefore, it seems that, in the gas phase, the intrinsic barriers to C–H bond scission are much smaller than the intrinsic barriers to C–H bond scission, independent of the chemical environment of the C–H and C–C bonds.

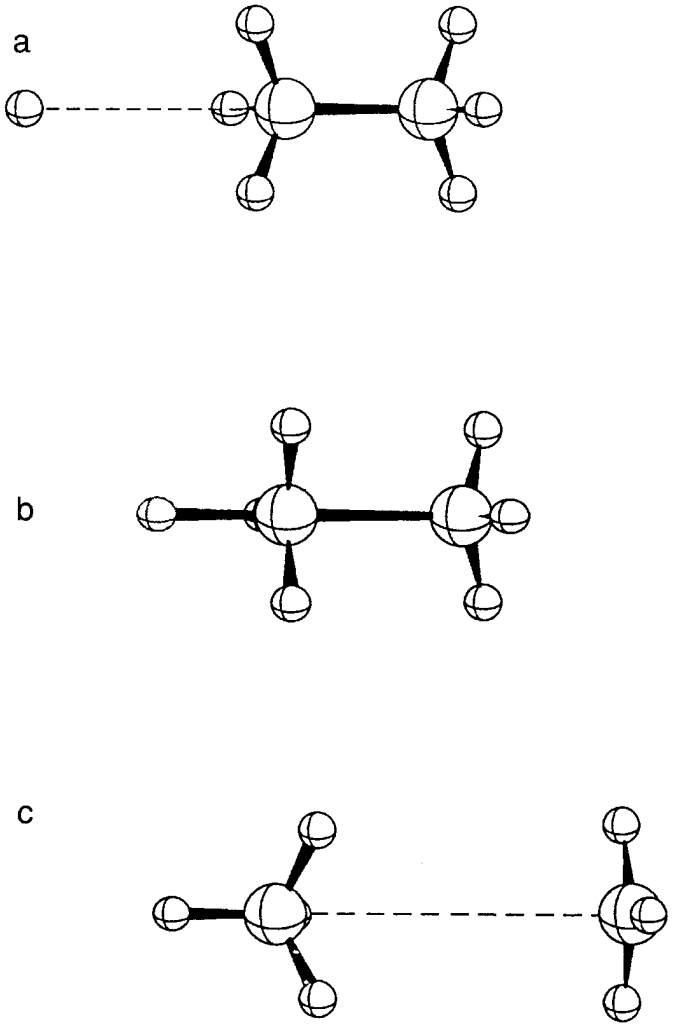

FIG. 5. The progress of the methyl transfer reaction, $H + C_2H_6 \rightarrow HCH_3 + CH_3$, with the deuterium approaching along the ethane's C–C bond.

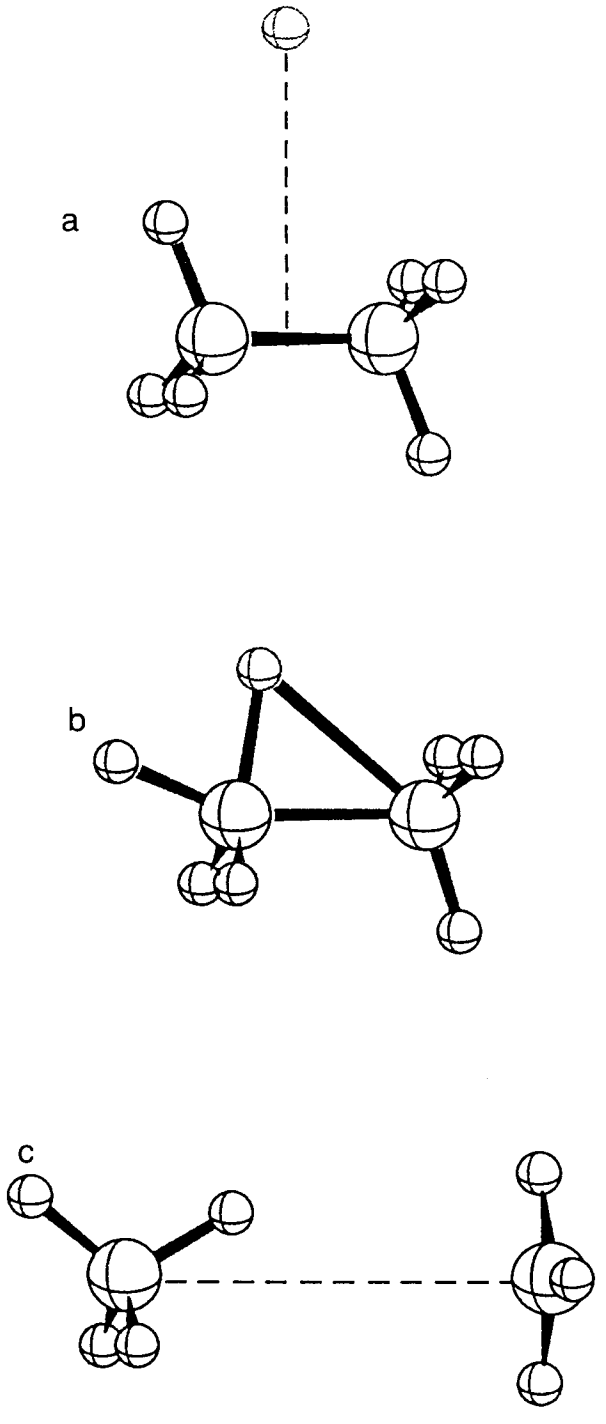

FIG. 6. The progress of the methyl transfer reaction, $H + C_2H_6 \rightarrow HCH_3 + CH_3$, with the deuterium approaching perpendicular to the ethane's C–C bond.

IMPLICATIONS AND SPECULATIONS

It is useful to consider what the results in the last section mean for catalysis. Notice that for all of the cases in Tables 2 and 3, the intrinsic barriers to C–H bond scission are about 30 kcal/mole lower than the intrinsic barriers to C–C bond scission. Therefore, one immediately knows that in the gas phase a hydrogenolysis reaction is inherently about 30 kcal/mole more difficult to accomplish than a hydrogenation/dehydrogenation reaction.

Such a result is quite important to gas-phase chemistry. Recall that most gas-phase reactions of the type $A_2 + B_2 \rightarrow 2AB$ go by radical propagation mechanisms, with an initiation step where radicals are formed

$$X + A_2 \rightarrow 2A\cdot + X, \qquad [5]$$

where X is a collision partner. A series of propagation steps, where radicals react with stable molecules,

$$A\cdot + B_2 \rightarrow AB + B\cdot \qquad [6]$$

$$B\cdot + A_2 \rightarrow AB + A\cdot \qquad [7]$$

and a recombination step where radicals are destroyed

$$X + 2A\cdot \rightarrow A_2X. \qquad [8]$$

Reactions [3] and [4] are both propagation steps where radicals react with stable molecules. Therefore, one key result of this paper is that propagation steps involving C–C bond scission have much higher intrinsic barriers than propagation steps involving C–H bond scission.

Laidler (15), Benson (16), and Hinshelwood (17) review the mechanisms of gas-phase reactions of hydrocarbons. Generally one finds that C–C bond scission can occur during the initiation step of a gas-phase reaction. However, all of the propagation steps in the reactions discussed in Laidler, Benson, and Hinshelwood go via a series of single atom transfers. C–C bond scission is not observed.

Westley (18) compiles data for over 1000 propagation reactions and about 200 initiation reactions of importance

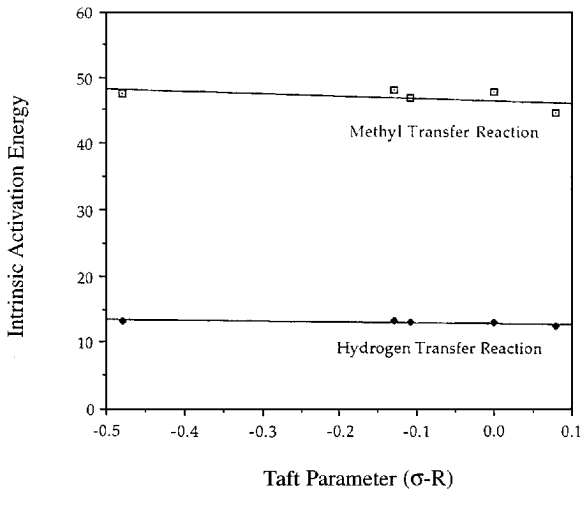

FIG. 7. The intrinsic activation energies as a function of the Taft Parameter, σ_R, for the different R groups.

to combustion. Again there are several examples of initiation reactions of the type $X + A_2 \rightarrow 2A + X$, where carbon–carbon bonds break during the collision of two stable molecules. However, of the 1000 plus propagation reactions only 8 involve C–C bond scission. In all of those 8 cases, the C–C bonds in the molecules are weak. We have used the Marcus equation to estimate the intrinsic barriers for these 8 cases, and find that in all of these cases the intrinsic barriers to C–H bond scission are considerably lower than the intrinsic barriers to C–C and C–O bond scission. Therefore, it seems that the calculations in this paper provide some interesting insights into the mechanisms of reactions in the gas phase.

It is useful to try to extend these results to surface reactions. It is important to say at the start that so far we have only done gas-phase calculations. One has to be cautious about using gas-phase calculation to predict things about surface reactions. One would expect there to be some changes in the intrinsic barriers when molecules are adsorbed on a surface. In particular, if we absorb species onto an insulator surface, all of the species will be charged. Charged species react very differently than radicals. On a transition metal surface, however, most of the species are neutral. The presence of the metal will still affect the intrinsic barriers. However, the effect would be expected to be much smaller than on an insulator surface.

One can use experimental data to provide an estimate of how much the intrinsic barriers change in moving from the gas phase to the surface. Consider comparing ethane hydrogenolysis

$$C_2H_6 + H_2 \rightarrow 2CH_4 \qquad [9]$$

to ethylene hydrogenation

$$C_2H_4 + H_2 \rightarrow C_2H_6. \qquad [10]$$

Previous workers have found the C–C bond scission is rate determining in reaction 9 while C–H bond formation in an ethyl species is rate determining in reaction 10. Reaction 9 has an activation barrier of 54 kcal/mole on a platinum catalyst while reaction 10 has a barrier of 9 kcal/mole. That means that reaction 9 has a 45 kcal/mole higher barrier than reaction 10. Reactions 9 and 10 are both exothermic. However, reaction 10 is 18 kcal/mole more exothermic than reaction 9. Plugging into Eq. [1], assuming $\gamma_P = 0.6$ shows that the intrinsic barrier to reaction 10 is 34 kcal/mole ($= 45$ k/cal/mole-0.6×18 kcal/mole) less than the intrinsic barrier for reaction 9. This compares favorably to the 33 kcal/mole we find in the gas phase.

The implication of this result is that while the individual intrinsic barriers change when one puts molecules on a transition metal surface, the difference in the intrinsic barriers changes to a much smaller extent. Therefore, there is the possibility that one can use gas-phase values of the intrinsic barriers to make useful predictions about surface reactions.

Just to see how this would work, in the remainder of the paper we will make the adhoc assumption that on a transition metal surface the intrinsic barriers to C–C and C–O bond scission are 20–40 kcal/mole larger than the intrinsic barriers to C–H bond scission and see if we can make useful predictions.

The first prediction is that, generally, when simple hydrocarbons and oxygenates decompose on transition metal surfaces in UHV, the molecules should usually decompose via a series of hydrogen transfer reactions and not a series of C–C bond scission reactions. This may seem to be a surprising prediction since C–C and C–O single bonds are weaker than C–H or O–H bonds in most hydrocarbons. However, the 20–40 kcal/mole difference in the intrinsic barriers is usually sufficient to make the activation barrier to C–H or O–H bond scission to be lower than the activation barrier to C–C or C–O bond scission. Yagasaki and Masel (19) and Davis and Barteau (20) review the mechanism of hydrocarbon and oxygenate decomposition on a variety of transition metal surfaces. Generally, most hydrocarbons decompose via sequential dehydrogenation with little C–C bond scission on all faces examined previously except (1×1) Pt(110). Methanol also decomposes via sequential dehydrogenation on all the metals examined previously except (1×1) Pt(110). With the exception of the Pt(110) data all of these results are fully consistent with the idea that the intrinsic barriers to C–C and C–O bond scission are considerably higher than the intrinsic barriers to C–H and O–H bond scission.

Ethanol follows a different pathway, however. First there are some sequential dehydrogenations, then the C–C bond breaks. Interestingly, however, one can predict the mechanism of ethanol decomposition on most transition metal surfaces by assuming the intrinsic barrier to C–H and O–H bond scission is 20–40 kcal/mole lower than the intrinsic barrier for C–C and C–O bond scission.

In principle, ethanol could decompose by a host of different reaction pathways. The ethanol can sequentially dehydrogenate. The C–O bond could break before any other reaction occurs. Now let us ask which reaction is most favored if the intrinsic barrier for the scission of a C–C or O–C bond is 20–40 kal/mole higher than the intrinsic barrier to the scission of a C–H or O–H bond. We will also assume that the intrinsic barriers to reaction rise substantially, if during the reaction, dangling bonds are produced far away from the surface. The latter assumption is discussed in Masel (1).

Figure 8 shows the bond energies in ethanol. Notice that the C–O bond is the weakest bond in the molecule. Therefore, if all of the intrinsic barriers to bond scission were equal, one would expect the C–O bond in ethanol to be easier to break than the C–H, O–H, and C–C bond. However, if one considers the difference in intrinsic barriers,

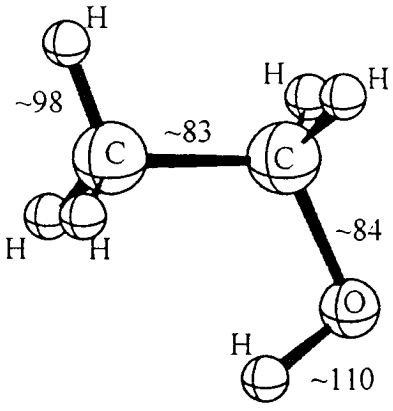

FIG. 8. The geometry and bond energies of ethanol.

one would come to a very different conclusion. If one assumes that the intrinsic barrier for the scission of a C–C or O–C bond is 20–40 kcal/mole higher than the intrinsic barrier to the scission of a C–H or O–H bond, then the C–O bond would be harder to break than either the O–H or C–H bond. Therefore, both the C–H or O–H bond should break at lower temperatures than the C–O bond.

Now consider whether the O–H or C–H bond should be easier to break. Notice that the C–H bond is weaker than the O–H bond. Therefore, based on bond energies alone, the C–H bond should break more easily than the O–H bond. However, if one looks at the reaction in detail one finds that there is what Masel (1) has called the proximity effect which substantially raises the intrinsic barrier for C–H bond scission. During C–H bond scission, the C–H bond breaks, and new carbon–surface and hydrogen–surface bonds form. Figure 9 shows a possible transition state for the reaction. Notice that it is hard to form a carbon surface bond because the carbon–hydrogen bonds get in the way. One does not know how much energy this costs without doing detailed calculations. However, the repulsions are similar to the extra repulsions in Fig. 6. In the calculations earlier in this paper, we found that such repulsions raise the intrinsic barriers by 24 kcal/mole.

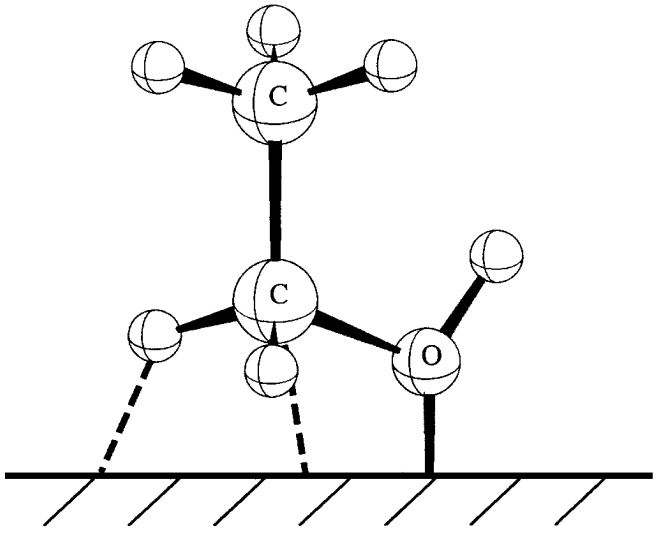

FIG. 9. A possible transition state for the C–H bond scission pathway of ethanol decomposition on a metal surface.

One can do the same analysis on the O–H bond scission step. In the case of O–H bond scission, there are some extra intrinsic barriers due to the repulsions of the empty dangling bonds on the ethanol. However, those effects would be expected to be much smaller than the extra 24 kcal/mole repulsion if the C–H bond breaks. Therefore, based on an analysis of the intrinsic barriers, one would expect O–H bond scission to have a lower activation barrier than C–H, C–C, or C–O bond scission, even though the O–H bond is the strongest bond in ethanol. Therefore, we conclude that based on a analysis of the intrinsic barriers, the first step in ethanol decomposition should be O–H bond scission to yield an ethoxy intermediate. That is what has been observed experimentally on all of or faces or all of the transition metals which have been examined previously except Pt(110) (2×1) and Pt(331).

One can continue the analysis to predict a mechanism of ethoxy decomposition on metals. Again, we note that the C–C bond in ethoxy is a bond 10 kcal/mole weaker than the C–H bond. Therefore, if one only considered bond energies, one would expect the C–C bond in ethoxy to break before the C–H bond. However, the intrinsic barriers go in the opposite directions. The intrinsic barriers for C–H bond scission are much lower than the intrinsic barriers for C–C bond scission. If one plugs numbers into Eq. [1], one finds that the overall activation barrier for ethoxy dehydrogenation should be 10–20 kcal/mole lower than the activation barrier for C–C bond scission in ethoxy. Consequently, the ethoxy should sequentially dehydrogenate to produce an acetaldehyde and an acetyl intermediate as indicated in Fig. 10.

The analysis changes after the acetyl intermediate forms. Note that if we use the analysis in Benziger (25), we find that on platinum, the reaction

$$CH_3CO_{ad} \rightarrow CH_{3\,ad} + CO_{ad} \qquad [11]$$

is favored by about 55 kcal/mole over the reaction

$$CH_3CO_{ad} \rightarrow H_{ad} + CH_2CO_{ad}. \qquad [12]$$

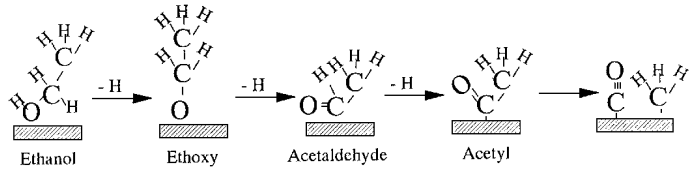

FIG. 10. Dehydrogenation of ethoxy to form acetaldehyde and an acetyl intermediate. A mechanism of ethoxy decomposition on metals.

Reaction 12 has a 20–40 kcal/mole lower intrinsic barrier than reaction 11, but that lower intrinsic barrier is overcome by the 55 kcal/mole extra driving force. Therefore, according to Eq. [1] reaction 11 should have a lower activation barrier than reaction 12. Consequently, one would expect the acetyl intermediate to decompose via reaction 11 rather than reaction 12. Experimentally one finds that ethoxy decomposition follows the mechanism in Fig. 10 in all of the cases examined so far, except in the case of ethoxy decomposition on Rh(100) where it appears that the sequence of dehydrogenation occurs in a different order.

At this point, there are only a couple of exceptions to these general guidelines. Wang and Masel (21) observed low-temperature C–O bond scission during Methanol decomposition on (1×1) Pt(110). Yagasaki and Masel (22) observed low-temperature C–C bond scission during ethylene decomposition on (1×1) Pt(110). Wang and Masel (23) and Cong, Van Spaendonk, and Masel (24) observed low-temperature C–O bond scission during ethanol decomposition on (2×1) Pt(110) and Pt(331). However, these systems are exceptions. The majority of the data in the literature are fully consistent with the assumption that the intrinsic barriers to C–C and C–O bond scission are 20–40 kcal/mole higher than the intrinsic barriers to C–H and O–H bond scission.

Admittedly, we have had to make a significant number of assumptions to obtain the values of the intrinsic barriers that we used in the above analysis. In particular we assumed that intrinsic barriers are similar in the gas phase and on a transition metal surface. We also assumed that the proximity effect is similar to the extra barriers we get when the reaction in Fig. 6 occurs. At this point, we have not justified these assumptions, and, in fact, would not expect these to be good assumptions on an insulating surface where species are charged. In a future paper we will find that in a carbenium ion, the intrinsic barriers to hydrogenolysis/isomerization are lower than the intrinsic barriers to hydrogenation/dehydrogenation. Still, the key point is that the intrinsic barriers allow us to quantify the idea that some reactions are harder than others. The intrinsic barriers, can be measured or calculated and one can use approximate values of the intrinsic barriers to predict the mechanisms of a wide variety of surface reactions.

CONCLUSIONS

In summary, in this paper we have proposed a simple heuristic to predict mechanisms of reactions: The intrinsic barriers to C–C and C–O bond scission are about 30 kcal/mole higher than the intrinsic barriers to C–H and O–H bond scission. We find that this heuristic is consistent with a wide variety of data in the literature, and our own *ab initio* calculations for gas-phase reactions. There are a few exceptions, though, all from experimental work from our own laboratory. Admittedly, the heuristic has not been fully tested experimentally or fully justified theoretically. However, it seems to give many useful results.

ACKNOWLEDGMENTS

This work was supported by the National Science Foundation under Grant CTS 94-03840. In this work we used the Silicon Graphics Power Challenge at the National Center for Supercomputing applications, University of Illinois, Urbana-Champaign.

REFERENCES

1. Masel, R. I., "Principles of Adsorption and Reaction on Solid Surfaces," Wiley, New York, 1996.
2. Evans, M. G., and Polayni, M., *Trans. Faraday Soc.* **32**, 133 (1936).
3. Marcus, R. A., *Disc. Faraday Soc.* **29**, 21 (1960).
4. Brønsted, J. N., and Pedersen, K., *Z. Phys. Chem.* **108**, 185 (1924).
5. Tempkin, M. I., and Pyzhev, U., *Acta Phys. Chem.* **12**, 327 (1940).
6. Balandin, A. A., *Adv. Catal.* **19**, 1 (1969).
7. Marcus, R. A., *J. Phys. Chem.* **72**, 891 (1968).
8. Curtiss, L. A., Raghavachari, K., Trucks, G. W., and Pople, J. A., *J. Chem. Phys.* **94**, 7221 (1991).
9. Schlegel, H. B., *J. Phys. Chem.* **92**, 3075 (1988).
10. Frish, M. J., Trucks, G. W., Schlegel, H. B., Gill, P. M. W., Johnson, B. G., Wong, M. W., Foresman, J. B., Robb, M. A., Head-Gordon, M., Replogle, E. S., Gomperts, R., Andres, J. L., Raghavachari, K., Binkley, J. S., Gonzalez, C., Martin, R. L., Fox, D. J., Defrees, D. J., Baker, J., Stewart, J. J. P., and Pople, J. A., GAUSSIAN 92/DFT, Revision G.2, Gaussian, Inc., Pittsburgh, 1993.
11. Frish, M. J., Trucks, G. W., Schlegel, H. B., Gill, P. M. W., Johnson, B. G., Robb, M. A., Cheeseman, J. R., Keith, T., Peterson, G. A., Montgomery, J. A., Raghavachari, K., Al-Laham, M. A., Zakrzewski, V. G., Ortiz, J. V., Foresman, J. B., Peng, C. Y., Ayala, P. Y., Chen, W., Wong, M. W., Andres, J. L., Replogle, E. S., Gomperts, R., Martin, R. L., Fox, D. J., Binkley, J. S., Defrees, D. J., Baker, J., Stewart, J. J. P., Head-Gordon, M., Gonzalez, C., and Pople, J. A., GAUSSIAN 94, Revision B.3., Gaussian, Inc., Pittsburgh, 1995.
12. Bockris, J. O' M., "Modern Electrochemistry," Vol. 2, p. 1110. Plenum, New York, 1970.
13. Gonzalez, C., and Schlegel, H. B., *J. Phys. Chem.* **94**, 5523 (1990).
14. Lee, W. T., and Masel, R. I., *J. Phys. Chem.* **99**, 9363 (1995).
15. Laidler, K. J., "Chemical Kinetics," Harper & Row, New York, 1987.
16. Benson, S. W., "Thermochemical Kinetics," Wiley, New York, 1976.
17. Hinshelwood, C. N., *The Kinetics of Chemical Change*, p. 364. Oxford Univ. Press, 1994.
18. Westley, F., "Table of Recommended Rate Constants for Chemical Reactions Occurring in Combustion," NBS, Washington, D.C., 1980.
19. Yagasaki, E., and Masel, R. I., *Catalysis* **111**, 1 (1994).
20. Davis, J. L., and Barteau, M. A., *Surf. Sci.* **187**, 387 (1987).
21. Wang, J., and Masel, R. I., *J. Am. Chem. Soc.* **113**, 5850 (1991).
22. Yagasaki, E., and Masel, R. I., *J. Am. Chem. Soc.* **112**, 8746 (1990).
23. Wang, J., and Masel, R. I., submitted for publication.
24. Cong, Y., van Spaendonk, V., and Masel, R. I., submitted for publication.
25. Benzinger, J., *in* "Metal Surface Reaction Energetics," (E. Shustorowch, Ed.), VCW, New York, 1991.